

Materials and methods

Materials. 1,2-dioleoyl-sn-glycero-3-phosphocholine (DOPC), brain and egg sphingomyelin (SM) and egg phosphatidylcholine (PC) were purchased from Avanti Polar Lipids. Cholesterol (Chol) was purchased from Sigma Aldrich. Two buffer solutions were freshly prepared and used as follows *i)* a fusion Buffer A containing 10 mM Tris, 150 mM NaCl 3 mM and CaCl₂ and *ii)* an imaging Buffer B of 10 mM Tris, 150 mM NaCl at pH 7.4. Buffer solutions were filtered before use with a 0.2 μm pore size inorganic membrane filter.

Preparation of supported lipid bilayers. DOPC, SM and Chol were dissolved in chloroform to give a final lipid concentration of 10 mM. Aliquots of DOPC and SM or Chol solutions were mixed in different DOPC:SM and DOPC:Chol molar ratios (either 70:30 or 50:50), poured into a glass vial and evaporated to dryness under a nitrogen flow. Multilamellar vesicles were obtained by hydration with the Buffer A solution to give a final lipid concentration of 1 mM and then subjecting the vial to 3 x 2.5 min cycles of tip sonication to obtain unilamellar vesicles.

Circular mica surfaces were used as substrates for AFM experiments. Prior to use, mica surfaces were glued onto Teflon discs with epoxy-based mounting glue. Phospholipid supported bilayers were prepared by the deposition of the small unilamellar vesicles suspension on freshly cleaved mica followed by incubation at 59°C. The samples were then slowly cooled to room temperature and thoroughly rinsed with Buffer B solution.

Toxin production, purification and validation. The SM-specific toxin fragment, non-toxic (NT) lysenin, was expressed in *E. coli* BL21 (DE3) as a fusion protein with a 6xHis-tag followed by the fluorescent protein mCherry (total MW ~45 kDa) at N-terminal, as purified and validated previously¹. The chol-specific toxin fragment, *i.e.* the fourth domain of perfringolysine (theta D4), was cloned in pET28 containing 6xHis- and LPETGG-tags in N- and C-terminal, respectively (Fig S1a). It was generated from pET28/His-mCherry-theta² by removing the mCherry sequence and adding the LPETGG-tag. The resulting plasmid was transformed in *E. coli* BL21 (DE3) and the protein expressed in LB medium for 72h at 16°C after addition of 0.4 mM isopropyl-β-D-thiogalactoside. Bacterial extracts and protein purification were prepared as previously described². Analysis of the purified protein by western blot revealed recombinant theta at the expected size (~16 kDa; Fig. S1b). The most enriched fractions were pooled, concentrated using Vivaspin turbo 15 columns (Sartorius), and the imidazole was removed by desalting on NAP-5 columns (GE Healthcare). Purified protein was finally kept in aliquots in 10 mM HEPES (pH 7.2) 10 mM NaCl and stored at -80°C until use. Protein concentration in the purified fraction was estimated by measuring A₂₈₀ and assuming a molar absorptivity of 44500 M⁻¹cm⁻¹. From 1 l of culture, we obtained 10 g of protein. The toxin binding specificity was verified on MLVs containing increasing amounts of Chol (Fig. S1b) and prepared as previously described¹.

AFM tip functionalization. Lysenin- and θ -functionalized AFM tips were obtained using NHS-PEG₂₇-acetal linkers³. To obtain NHS-PEG₂₇-acetal tips, AFM cantilevers were first cleaned with chloroform for 10 min, rinsed with ethanol, N₂ dried and then cleaned for 15 min in an ultraviolet radiation and ozone cleaner (UV-O, Jetlight, CA, USA). The cantilevers were immersed in an ethanolamine solution (3.3 g ethanolamine in 6.6 ml DMSO) overnight and then rinsed in DMSO (3 x 1 min) and ethanol (3 x 1 min), followed by N₂ drying. To attach the linker to the AFM tip, 1 mg of NHS-PEG₂₇-acetal was diluted in 0.5 ml chloroform with 30 μ l triethylamine and cantilevers were immersed in this solution for 2 h. The cantilevers were then cleaned 3 x 10 min in chloroform and dried with N₂. Next, the cantilevers were immersed in a 1% citric acid solution for 10 minutes and rinsed with pure water (3 x 5 min), followed by drying with N₂.

To obtain Lysenin-tips, 100 μ l of a 100 μ M tris-nitrilotriacetic amine trifluoroacetate (tris-NTA) solution was pipetted onto the cantilevers and 2 μ l of a freshly prepared 1 M NaCNBH₃ solution was then added and gently mixed. The cantilevers were incubated for 1 h, then 5 μ l of a 1 M ethanolamine solution pH 8.0 were added for 10 minutes to quench the reaction. Cantilevers were washed in Tris buffer (3 x 5 min) and then incubated for 1.5 h with 100 μ l of a 10 μ M Lysenin solution. Lysenin-tips were rinsed with Tris buffer and stored in individual wells of a multiwell dish until used in AFM experiments (typically within 48 h).

θ -functionalized AFM tips were obtained by incubating NHS-PEG₂₇-acetal cantilevers in 100 μ l of a 1 mM GGGGGGGGGGK peptide (Gly₁₀Lys, Genscript, USA) solution to which 2 μ l of a freshly prepared 1 M NaCNBH₃ solution was added. After 1 h, then 5 μ l of a 1 M ethanolamine solution pH 8.0 were added for 10 minutes to quench the reaction. Cantilevers were then incubated with 20 μ l of a 10 μ M θ -toxin solution and 20 μ l of a 10 μ M Sortase A solution for 1 h at 37°C. θ -tips were rinsed with Tris buffer and stored in individual wells of a multiwell dish until used in AFM experiments the same day.

FD-based AFM on supported lipid bilayers. AFM experiments were performed with a Bioscope Resolve AFM (Bruker) operated in “PeakForce Tapping QNM mode” in imaging Buffer B at room temperature (\approx 24°C). Rectangular Si₃N₄ cantilevers (AC40, Bruker) with a sharpened tetrahedral silicon tip, nominal spring constants of 0.09 N/m and resonance frequency in liquid of \approx 25 kHz were used. The spring constant of the cantilevers was calibrated using the thermal noise method at the end of each experiment⁴ and was found to be of 0.08 ± 0.01 N/m.

In FD-based AFM measurements, the AFM cantilever is oscillated well below its resonance frequency in a sinusoidal manner, while the sample surface is contoured pixel-by-pixel. A force-distance curve is recorded for each approach and retraction of the oscillating cantilever. FD-based AFM height, Young’s modulus and adhesion maps are then obtained by doing a pixel-by-pixel reconstruction of the acquired data. FD-based multiparametric maps were acquired using a force setpoint of 100-200

pN. The AFM cantilever was oscillated vertically at 0.25 kHz with peak-to-peak oscillation amplitudes of 100 nm. Images were recorded using a scan rate of 0.2 Hz and 256x256 pixels.

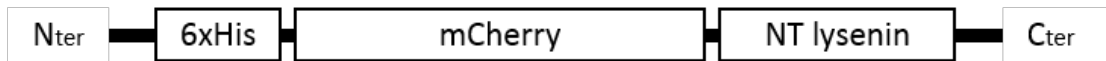
Data analysis. Raw FD curves were processed offline using the NanoScope Analysis 1.80 Software (Bruker). To reconstruct Young's modulus maps, we analyzed the approach part of the force-distance curves from PeakForce QNM maps. The best quality of the fit was obtained when by fitting the contact part of the curve with the Hertz model^{5,6}:

$$F^{2/3} = \left(\frac{4}{3} \frac{E}{(1-\nu^2)} \sqrt{R} \right)^{2/3} \delta \quad (1)$$

where E is the Young's modulus, δ is the indentation depth, ν is the Poisson ratio, and R is the contact radius. We used a Poisson's ratio value of 0.3. Young's modulus was calculated from the slope of Equation 1.

Height images were processed using the Gwyddion free SPM software. A first or second order plane fit was performed. Images did not undergo further processing.

a lysenin toxin fragment



theta toxin fragment



b

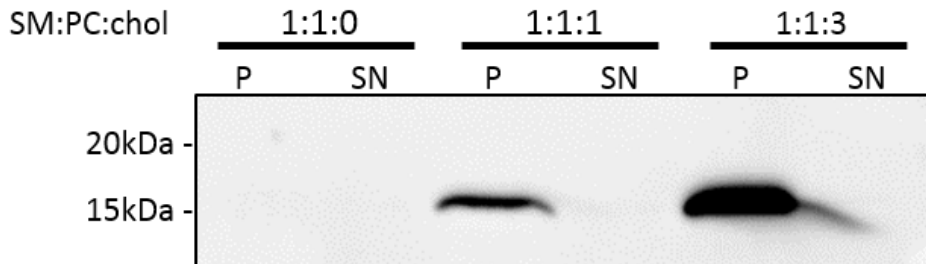


Fig. S1. Toxin fragment production (a) and validation of the theta toxin fragment (b). (a) Mapping of pET28-expressing lysenin or theta toxin. (b) Theta toxin fragment (16 kDa) binding specificity validation on multilamellar vesicles (MLVs) containing increasing Chol contents. Theta was incubated with MLVs made of SM and PC and containing (4 last wells) or not (2 first wells) Chol. After centrifugation, pellets (P) containing MLVs and supernatants (SN) were analysed by western blotting using anti-His antibodies. The 6xHis-tagged toxin only binds Chol-containing MLVs (P).

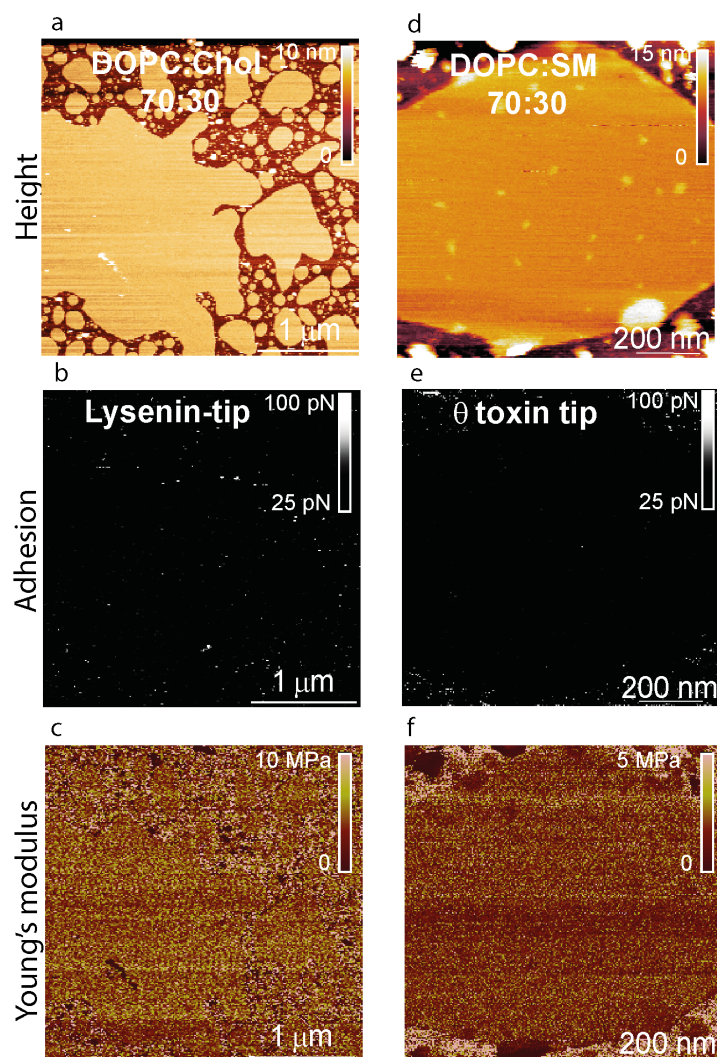


Fig. S2. Validating the specificity of the interactions detected by toxin-derivatized AFM tips. The lysenin-tip was used to probe a SM-free lipid bilayer of DOPC:Chol (70:30). (a,b,c) Height, adhesion and Young's modulus images of the DOPC:Chol (70:30). No specific unbinding event were observed between the Lysenin-tip and the DOPC:Chol sample. (d,e,f) A θ -functionalized AFM tip was used to map a Chol-free lipid bilayer made of DOPC:SM (70:30) (d) High-resolution height image of the DOPC:SM (70:30) bilayer and (e) corresponding adhesion showing no interaction between the tip and the sample and (f) Young's modulus map

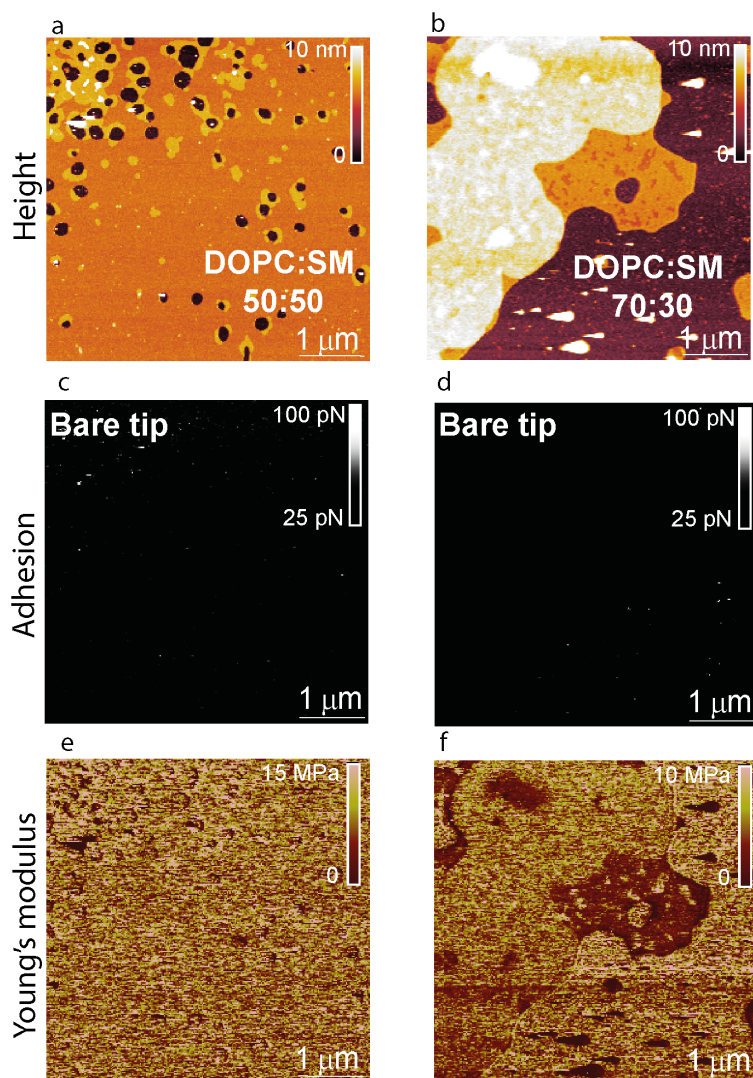


Fig. S3. Mapping SM-enriched domains with bare AFM tips on DOPC:SM 50:50 and 70:30 lipid bilayers. (a,b) Height images of the bilayers and corresponding (c,d) adhesion and (e,f) Young's modulus maps.

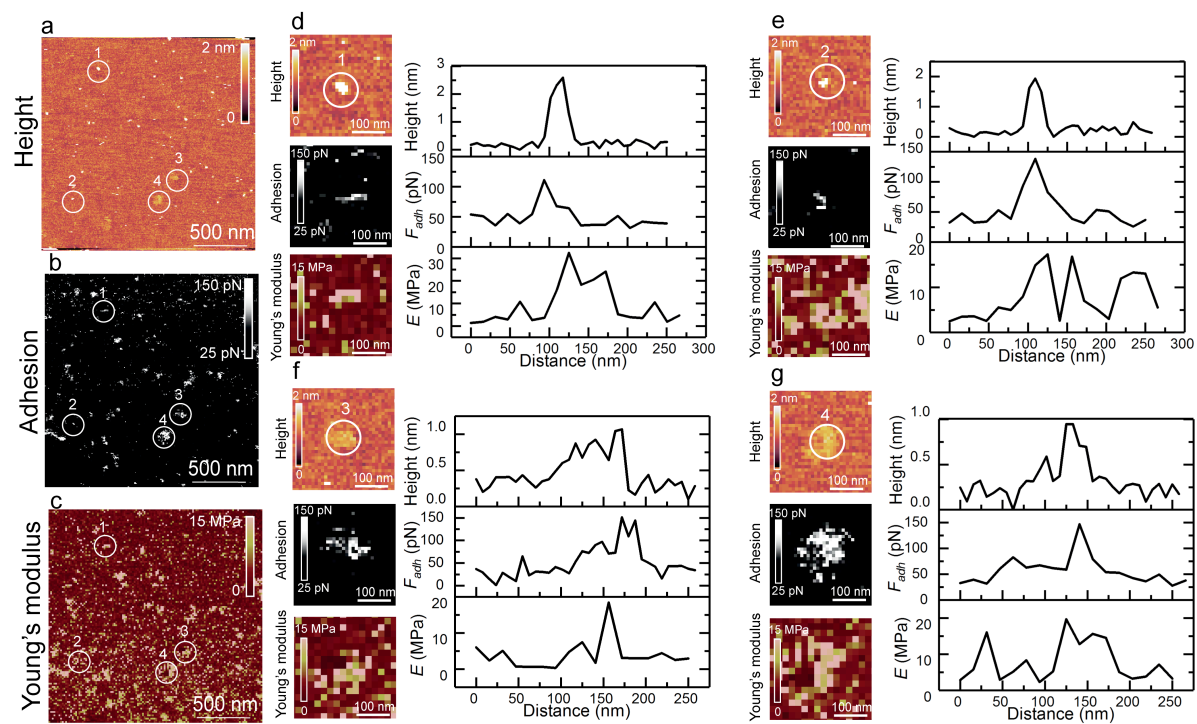


Figure S4. Mapping Chol-enriched domains with a θ -functionalized AFM tip on a DOPC:Chol (70:30) lipid bilayer. (a) High-resolution height image of the bilayer and (b,c) corresponding adhesion and Young's modulus maps. (d-f) Higher magnification maps of single Chol-enriched domains encircled in (a-c) along with the corresponding height, adhesion force and Young's modulus (E) cross-section profiles.

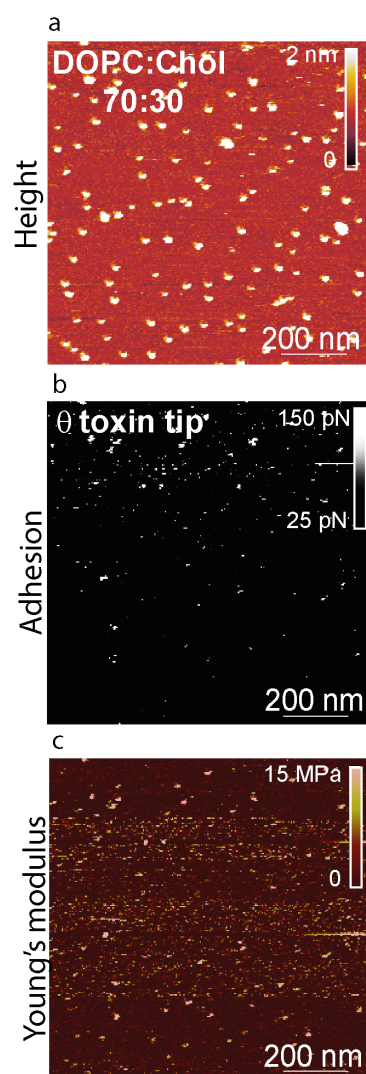


Fig S5. Mapping Chol-enriched domains with a θ -functionalized AFM tip on a DOPC:Chol (70:30) lipid bilayer. (a) High-resolution height image of the bilayer and (b,c) corresponding adhesion and Young's modulus maps.

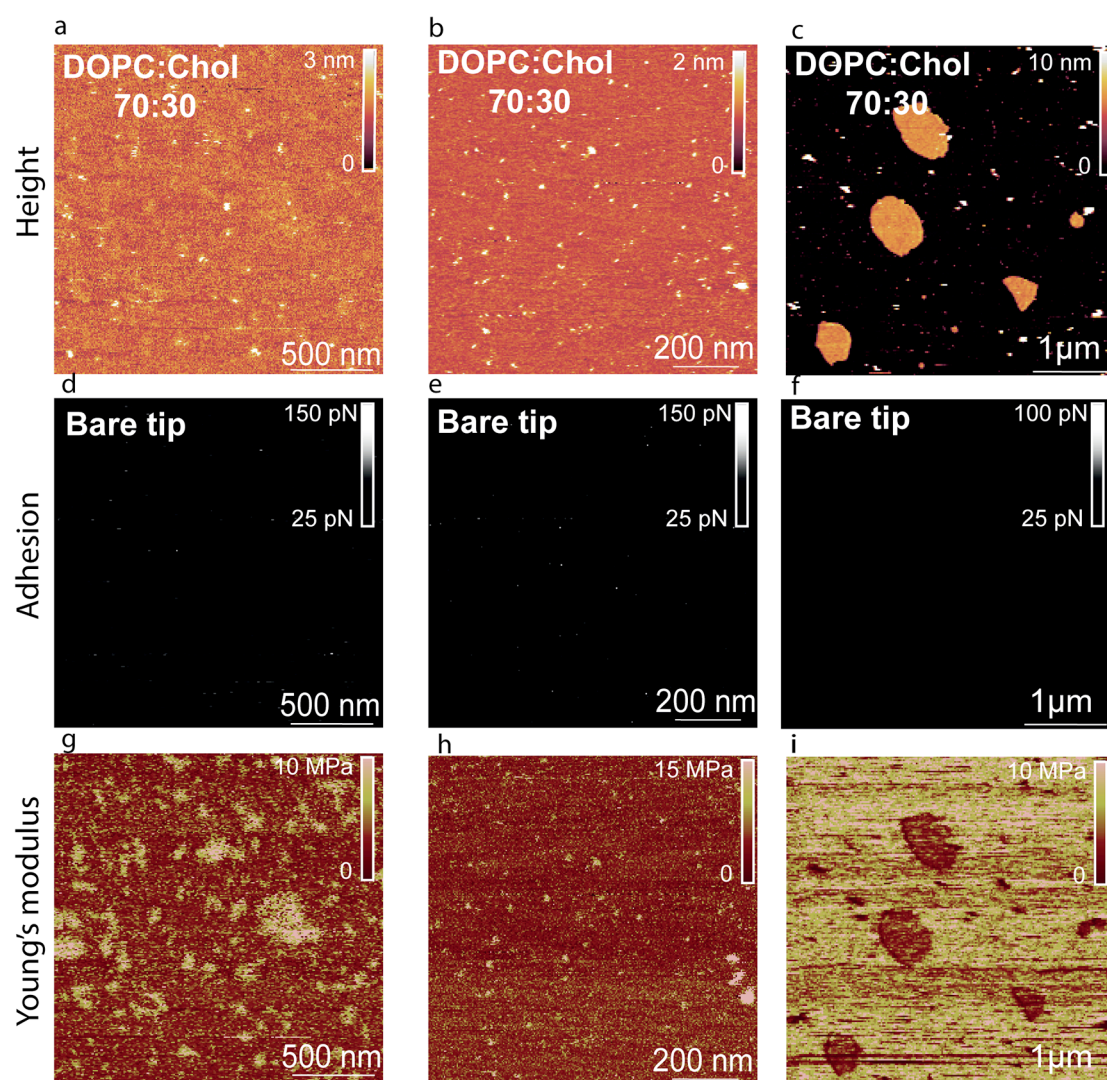


Fig. S6. Mapping Chol-enriched domains with a bare AFM tip on DOPC:Chol 50:50 and 70:30 lipid bilayers. (a,b,c) Height images of the bilayers and corresponding (d,e,f) adhesion and (g,h,i) Young's modulus maps.

References

1. M. Carquin, H. Pollet, M. Veiga-da-Cunha, A. Cominelli, P. Van Der Smissen, F. N'kuli, H. Emonard, P. Henriët, H. Mizuno, P. J. Courtoy and D. Tyteca, *Journal of Lipid Research*, 2014, **55**, 1331-1342.
2. M. Carquin, L. Conrard, H. Pollet, P. Van Der Smissen, A. Cominelli, M. Veiga-da-Cunha, P. J. Courtoy and D. Tyteca, *Cellular and Molecular Life Sciences*, 2015, **72**, 4633-4651.
3. L. Wildling, B. Unterauer, R. Zhu, A. Rupprecht, T. Haselgrübler, C. Rankl, A. Ebner, D. Vater, P. Pollheimer, E. E. Pohl, P. Hinterdorfer and H. J. Gruber, *Bioconjugate Chemistry*, 2011, **22**, 1239-1248.
4. J. L. Hutter and J. Bechhoefer, *Review of Scientific Instruments*, 1993, **64**, 1868-1873.
5. H. Schillers, C. Rianna, J. Schäpe, T. Luque, H. Doschke, M. Wälte, J. J. Uriarte, N. Campillo, G. P. A. Michanetzis, J. Bobrowska, A. Dumitru, E. T. Herruzo, S. Bovio, P. Parot, M. Galluzzi, A. Podestà, L. Puricelli, S. Scheuring, Y. Missirlis, R. Garcia, M. Odorico, J.-M. Teulon, F. Lafont, M. Lekka, F. Rico, A. Rigato, J.-L. Pellequer, H. Oberleithner, D. Navajas and M. Radmacher, *Scientific Reports*, 2017, **7**, 5117.
6. H. Hertz, *Journal für die reine und angewandte Mathematik*, 1882, **92**, 156-171.